Front. Environ. Sci. Eng. 2015, 9(5): 823–831
DOI 10.1007/s11783-015-0787-9

RESEARCH ARTICLE

Interaction of carbonaceous nanomaterials with wastewater biomass

Yu YANG (✉)[1], Zhicheng YU[1], Takayuki NOSAKA[2], Kyle DOUDRICK[3], Kiril HRISTOVSKI[4], Pierre HERCKES[5], Paul WESTERHOFF[1]

1 School of Sustainable Engineering and the Built Environment, Arizona State University, Tempe, AZ 85287, USA
2 School for Engineering of Matter, Transport and Energy, Arizona State University, Tempe, AZ 85287, USA
3 Department of Civil and Environmental Engineering and Earth Sciences, University of Notre Dame, Notre Dame, IN 46556, USA
4 The Polytechnic School, Arizona State University, Mesa, AZ 85212, USA
5 Department of Chemistry and Biochemistry, Arizona State University, Tempe, AZ 85287, USA

Abstract Increasing production and use of carbonaceous nanomaterials (NMs) will increase their release to the sewer system and to municipal wastewater treatment plants. There is little quantitative knowledge on the removal of multi-walled carbon nanotubes (MWCNTs), graphene oxide (GO), or few-layer graphene (FLG) from wastewater into the wastewater biomass. As such, we investigated the quantification of GO and MWCNTs by UV-Vis spectrophotometry, and FLG using programmable thermal analysis (PTA), respectively. We further explored the removal of pristine and oxidized MWCNTs (O-MWCNTs), GO, and FLG in a biomass suspension. At least 96% of pristine and O-MWCNTs were removed from the water phase through aggregation and 30-min settling in presence or absence of biomass with an initial MWCNT concentration of 25 $mg \cdot L^{-1}$. Only 65% of GO was removed with biomass concentration at or above 1,000 $mg \cdot L^{-1}$ as total suspended solids (TSS) with the initial GO concentration of 25 $mg \cdot L^{-1}$. As UV-Vis spectrophotometry does not work well on quantification of FLG, we studied the removal of FLG at a lower biomass concentration (50 mg $TSS \cdot L^{-1}$) using PTA, which showed a 16% removal of FLG with an initial concentration of 1 $mg \cdot L^{-1}$. The removal data for GO and FLG were fitted using the Freundlich equation (R^2 = 0.55, 0.94, respectively). The data presented in this study for carbonaceous NM removal from wastewater provides quantitative information for environmental exposure modeling and life cycle assessment.

Received December 24, 2014; accepted March 25, 2015

E-mail: yu.yang.2@asu.edu

Keywords multi-walled carbon nanotubes, graphene oxide, graphene, removal, wastewater biomass

1 Introduction

Carbon nanotubes (CNTs) and graphene are increasingly incorporated in consumer products and industrial processes, including flame retardant materials [1], aerospace materials [2], and other applications [3]. These carbonaceous nanomaterials (NMs) are mainly composed of aromatic carbon structure with or without surface functionalization [3]. Multi-walled CNTs (MWCNTs) are the most dominant and representative class of these carbonaceous NMs [4], and their estimated production is 55–1,101t·$year^{-1}$ [5]. Although there are no substantiated reports confirming the annual production of graphene on a global scale, the graphene market is anticipated to reach $149.9 million by 2020 [6]. This rapid growth in carbonaceous NM production and markets will inevitably increase their release into the environment.

Nanomaterial release to the environment occurs throughout all life cycle stages, starting with synthesis and purification, incorporation into products, recycling of manufacturing waste, product usage, and ending with disposal [3,7]. NMs released to wastewater eventually enter wastewater treatment plants (WWTPs). As such, the NM manufactures in the United States must consider discharges of NMs to sewers and removal at WWTPs. However, limited information exists about the removal of MWCNTs and graphene in WWTPs [3]. Modeling results estimate that MWCNTs are released to receiving waters at low concentrations (i.e., less than 1 $mg \cdot L^{-1}$) [8,9]; however the ability of WWTPs to remove carbonaceous NMs needs to be verified. In the absence of data,

manufacturers must assume zero NM removal from water across WWTPs in the United States [10]. Exploring the removal of carbonaceous NMs by municipal WWTPs is necessary to close the knowledge gap.

The main challenge of determining NM removal stems from barriers to quantifying NMs in wastewater or biomass matrices. Until recently, measuring carbonaceous NMs other than fullerene (C_{60}) derivatives by mass spectroscopy methods has not been reported [11]. Single-walled CNTs were recently measured using single particle inductively coupled plasma mass spectrometry (ICP-MS), where catalysts in the single-walled CNTs (e.g., yttrium) were surrogates for the CNTs, but this is not feasible with most multi-wall CNTs because they use more earth abundant metals in mass which can cause background interference. MWCNTs with unique isotopic carbon ratios have been quantified using combustion followed by mass spectroscopy [12], which cannot be applied in our study due to the complicated background carbon in the biomass. We and others have developed a programmable thermal analysis (PTA) method for MWCNTs [13] and have applied this method to quantify MWCNTs in rat lung tissue [14] and graphene oxide (GO) in biomass [15]. When using PTA to quantify carbonaceous NMs in complex organic matrices, removal or digestion of background carbon is required to reduce carbon interference or false positives. We have demonstrated PTA to analyze graphene in matrix with low biomass concentration (e.g., 50 mg·L^{-1}, total suspended solids, TSS). However, challenges still existed when analyzing MWCNTs and GO in the presence of high biomass concentration (e.g., $\geqslant$1,000 mg TSS·L^{-1}). Alternatively, as will be discussed below, MWCNTs and GO are easily dispersed in solution and yield UV-Vis absorption spectra [15] that did not interfere with soluble organics, allowing UV-Vis to be used for quantification of the supernatant mass of MWCNTs and GO.

The aim of this study was to determine the removal of carbonaceous NMs by the wastewater biomass, including MWCNTs, GO, and graphene. Batch biosorption studies were conducted in a range of biomass concentration (e.g., 50 – 3,000 mg TSS·L^{-1}). The mass of carbonaceous NMs adsorbed to biomass or retained in the liquid was quantified by UV-Vis or PTA method. Results obtained from this study provide critical information in environmental assessment and environmental exposure modeling [8,9].

2 Experimental approach

2.1 Preparation and characterization of carbonaceous nanomaterials dispersions

GO suspension was obtained from TW Nano Materials (CA, USA) with the following characteristics provided by the manufacturer: 0.2 wt.%, $>$90% single layer, 0.5 – 20 μm in *x*–*y*, 1.1 nm of thickness when dispersed in water, 1:1.3 C:O ratio, $>$1,200 m^2·g^{-1}). Because single-layer, non-oxidized graphene is hard to achieve in aqueous solution, few-layer graphene(FLG) nanoplatelet powder (N006-P, Angstron Materials, OH, USA) was chosen to represent graphene and was used as received (characteristics by manufacture: $>$97% carbon, $<$1.5% oxygen, $<$1.5% ash, 10–20 nm thick, $<$14 μm in *x*–*y* 122 direction, 21 m^2·g^{-1}) [15]. MWCNTs (length 5-20 μm, outer diameter 15±5 nm) were obtained from Nanolab Technologies (Milpitas, CA, USA) and oxidized by researchers in the laboratory of Dr. Howard Fairbrother at Johns Hopkins University [16]. Briefly, MWCNTs were oxidized in a concentrated acid mixture of sulfuric acid (98% H_2SO_4 by mass) and nitric acid (69% HNO_3 by mass) at 70°C for 8 h and in a volume ratio of sulfuric acid to nitric acid of 3:1 [17]. After further washing (with deionized water) and drying, four types of MWCNTs were characterized by X-ray photoelectron spectroscopy (XPS) and showed surface oxygen contents of 3.5%, 6.4%, 7.3%, 8.3% [18]. As the surface oxygen content in pristine MWCNTs was 0.4%, which was below 2% and considered as common pristine MWCNTs [16]. The MWCNTs with higher oxygen contents (i.e., 3.5%–8.3%) were considered to be oxidized MWCNTs (O-MWCNTs) [16]. The dispersion of both pristine and O-MWCNTs was sonicated in a water bath sonicator for one hour, and the GO suspension was sonicated for 5 min before using. The final concentrations used for all experiments were 25 mg MWCNTs·L^{-1}and 25 mg GO·L^{-1}.

2.2 Carbonaceous nanomaterials removal experiments

The removal of carbonaceous NMs from wastewater liquid by wastewater biomass was examined following experimental protocols by Kiser et al. [19]. In brief, clean activated sludge was collected from a laboratory-scale sequencing batch reactor seeded by activated sludge from a local WWTP. The continuous two year operation of the reactor ensures that the biomass is not externally contaminated by metals or carbonaceous NMs. Collected biomass was refrigerated at 4°C and stored for less than 24 h before use. Prior to experiments, activated sludge was rinsed three times with a carbonate buffer solution (10 mmol·L^{-1} NaCl and 4 mmol·L^{-1} $NaHCO_3$) and then centrifuged (F = 350 G) for 15 min. The supernatant was discarded, and dewatered sludge was re-suspended in a 1 mmol·L^{-1} of $NaHCO_3$ buffer solution. The pH of mixed sludge and buffer solution was adjusted to pH 7.0±0.2 with 0.1 mmol·L^{-1} of HCl or 0.1 mmol·L^{-1} of NaOH. After pH adjustment, the TSS of the biomass stock solution was determined using standard method [20].

Aliquots of biomass stock solution were spiked into a series of plastic vials containing NMs and buffered with 1 m mol·L^{-1} $NaHCO_3$ solution. The final biomass concentration ranged from 50 mg TSS·L^{-1} to 3,000 mg

$TSS \cdot L^{-1}$, where the maximum biomass concentration used in this study is similar to the typical activated sludge concentration in a WWTP [21]. Positive controls included NMs and buffer solution without biomass, and the negative control included only clean biomass and buffer solution. The final volume of all aliquots was 30 mL. The initial concentrations in the mixed liquor were 25 mg $GO \cdot L^{-1}$and 25 mg $MWCNTs \cdot L^{-1}$.

After mixing NMs and biomass, the suspensions were capped in tubes and agitated on a wrist-action shaker for 3 h, which is a typical duration for the aeration stage in a WWTP. Following agitation, the mixed suspension was settled by gravity for 30 min [19]. For GO and CNT experiments, a supernatant aliquot of 6 mL was pipetted out from each vessel for further analysis. The supernatant was centrifuged for 5 min at F = 1,000 G to remove any remaining suspended particles and then analyzed by UV-Vis method.

Experiments with FLG and clean biomass followed the same protocols except that different NM concentrations were used. To facilitate analysis, the initial concentrations of FLG ranged from 0.3 to 8.3 mg $Carbon \cdot L^{-1}$ (i.e., $C \cdot L^{-1}$). A single biomass concentration of 50 mg TSS $\cdot L^{-1}$was applied for all the FLG experiments. The negative control contained only biomass without any FLG. After 3 h of mixing and 30 min of gravity settling, 26 mL of supernatant was carefully removed with a pipette. The remaining suspension of 4 mL was centrifuged at F = 21,293 G for 10 min, and the supernatant was discarded. The remaining biomass was used for PTA analysis.

2.3 Quantification of the carbonaceous nanomaterials

MWCNTs and GO in the supernatant were quantified using a UV-Vis light scattering spectrophotometer (MultiSpec-1501, Shimadzu, Japan) with minimum detection limit of 1 $mg \cdot L^{-1}$. For FLG studies, biomass was digested in alkaline solution to eliminate excess biomass and facilitate separation of FLG before it was quantified using PTA [15]. The detailed PTA analysis is described by Doudrick et al. [13,15]. Briefly, 1 mL of SOLVABLE™ (aqueous based solubilizer, PerkinElmer, MA, USA) was added to the biomass remaining after centrifugation. The mixture was then incubated for 24 h at 60°C, and then 2% (by weight) of sodium borohydride (99.99%, Sigma Aldrich, MO, USA) was added to the mixture. To remove any residual surfactant from SOLVABLE™, the rinsing procedure consisted of centrifugation at F = 21,293 G for 10 min followed by decanting and addition of 1 mL of nanopure™ water (Barnstead, 18.2MΩ·cm). The suspension was agitated for 1 min using a vortex agitator, and then the centrifugation step was repeated. After centrifugation and removal of the supernatant, the final pellet that formed at the bottom of the centrifuge tube was suspended in 0.1 mL of nanopure water and used for PTA analysis.

2.4 Statistical analysis

Linear regression was conducted to calculate the coefficients of linear form of the Freundlich equation, using Microsoft Excel 2007. The value of R^2 was presented as a measure of goodness-of-fit of linear regression.

3 Results and discussion

3.1 Carbonaceous nanomaterial analysis in presence of wastewater biomass

In the wastewater biomass experiments, it was possible to measure NMs either in solution or in the biomass to calculate the removal of NMs from the liquid phase. However, both measurements face potential interferences when analyzing elemental carbon (i.e., NMs) in the presence of large amounts of dissolved and/or particulate organic matter associated with soluble microbial products (SMPs), cellular debris, and/or intact cells. Because NMs in supernatant are representative of the discharge from a full scale WWTP into receiving water, we preferred analyzing NMs in the supernatant when possible.

To identify the specific wavelength for quantification, UV-Vis spectra between 200 and 700 nm were obtained for three suspensions of NMs and the supernatant of biomass and are shown in Fig. 1(a). In the absence of NMs, soluble organics in a supernatant sample collected from a test with 1,000 mg $TSS \cdot L^{-1}$had minimal UV-Vis response at wavelengths longer than 300 nm. Thus absorbance at wavelengths equal to or above 300 nm can be used to quantify the concentration of NMs without the interference from biomass. GO exhibited peaks at both 230 and 300 nm, which were also observed in other studies [22,23]. To avoid interference from biomass supernatant background, 300 nm was used for GO quantification. No obvious peak was observed for the suspension of MWCNTs, and the wavelength of 400 nm was applied for quantification as it showed a large absorbance value.

Calibration curves were obtained by using UV-Vis for both GO and MWCNTs with a minimum detection limit of 1 $mg \cdot L^{-1}$ (Fig. 1 (a)). Pristine and O-MWCNTs with lower oxygen content (i.e., ⩽7.3%) were not as stable as O-MWCNTs with 8.3% of oxygen; the former quickly aggregated and precipitated in nanopure water or 1 mmol $\cdot L^{-1}$ $NaHCO_3$ even after a 1 h water bath sonication. Five types of MWCNTs were tested in this study, while O-MWCNTs with 8.3% of oxygen were quantifiable using a UV-Vis calibration curve. In the removal experiments, negative controls without NMs were conducted over a wide range of biomass concentrations (50 to 3,000 mg TSS $\cdot L^{-1}$). By subtracting the absorbance of the background biomass supernatant, the concentrations of GO or O-MWCNTs in supernatant could be quantified using UV-Vis absorption at 300 nm for GO and 400 nm for O-MWCNTs.

FLG at 20 mg·L^{-1} showed no specific absorption/scattering peak, and the highest absorbance between 200 and 700 nm was approximately 0.12 at 400 nm. Also, the concentration of FLG in the supernatant after biosorption was expected to very low, and challenges existed to collect and analyze FLG in supernatant. As such, instead of using the UV-Vis method described previously, PTA was used to quantify FLG because it has a lower detection limit. As a result, we quantified FLG in settled biomass instead of the supernatant. Figure 1(b) illustrates a typical PTA thermogram on FLG in biomass. When the amount of biomass was below 50 mg TSS·L^{-1}, the peaks on the left attributed from biomass in Fig. 1(b) was negligible. Thus 50 mg TSS·L^{-1} biomass led to no observable interference on the signal from FLG and was chosen for FLD distribution study in our research.

3.2 Removal of carbon nanotubes by wastewater biomass

Figure 2 shows the UV-Vis spectra for the experiment with the highest oxygen containing O-MWCNTs (i.e., the most stable MWCNT) at time zero and after the test (3 h mixing followed by 30 min gravity settling). The O-MWCNTs were well dispersed after the water-bath sonication after a water-bath sonication. In the positive control (i.e., without biomass), the absorbance was near zero wavelengths above 250 nm, indicating complete removal of the O-MWCNTs is simply due to homo-aggregation and sedimentation. Visual observations showed a clear supernatant, thus supporting the conclusions of the UV-Vis measurements. The same process was repeated for the other three O-MWCNTs and pristine MWCNTs. We visually observed more rapid aggregation as the oxygen content of the

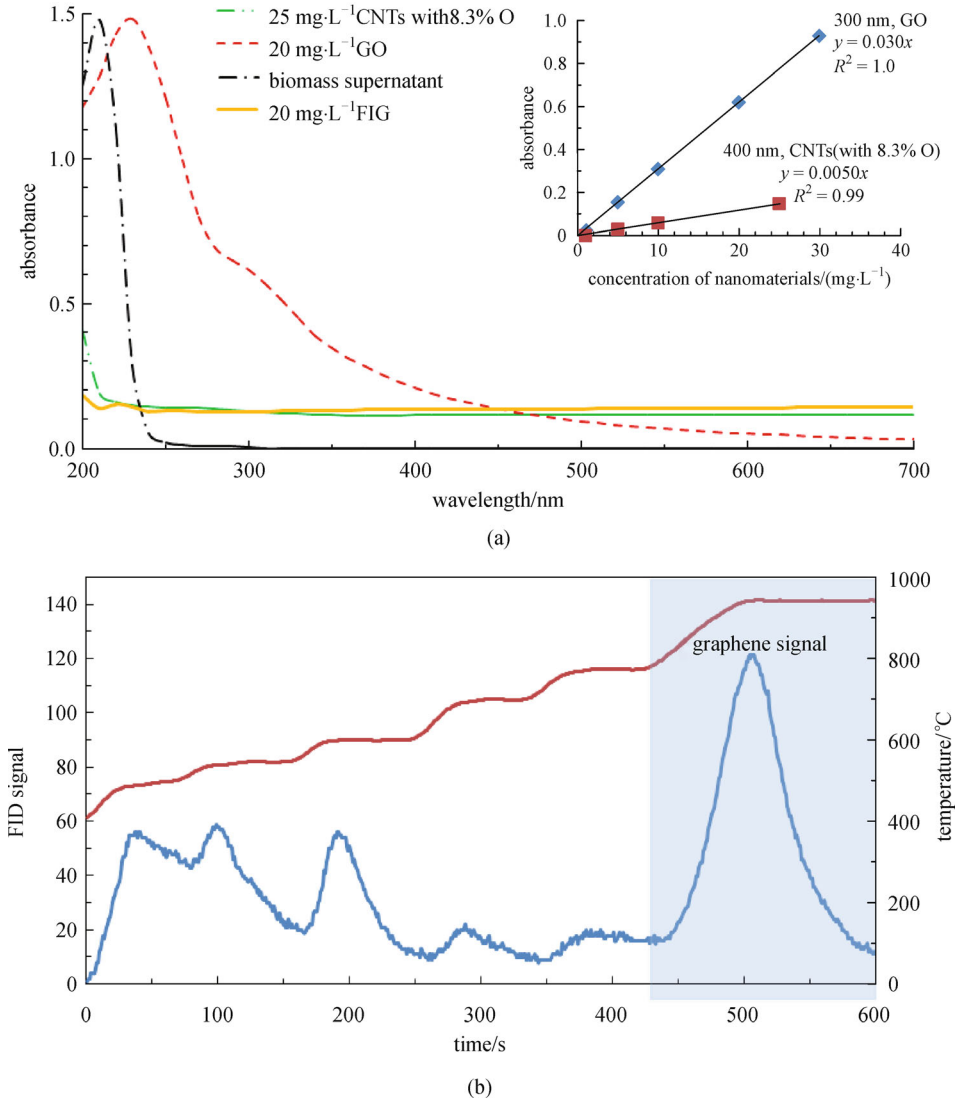

Fig. 1 (a) UV-Vis characterization of graphene oxide (GO) suspension (20 mg·L^{-1}), carbon nanotubes with surface oxygen content of 8.3% (25 mg·L^{-1}), and biomass supernatant (after 30 minutes settling of 1,000 mg·L^{-1} biomass). (b) PTA thermogram for adsorption test of FLG in biomass under He/O_2 atmosphere. Signal in shaded area (> 775 °C) is counted for FLG quantification of 50 μg

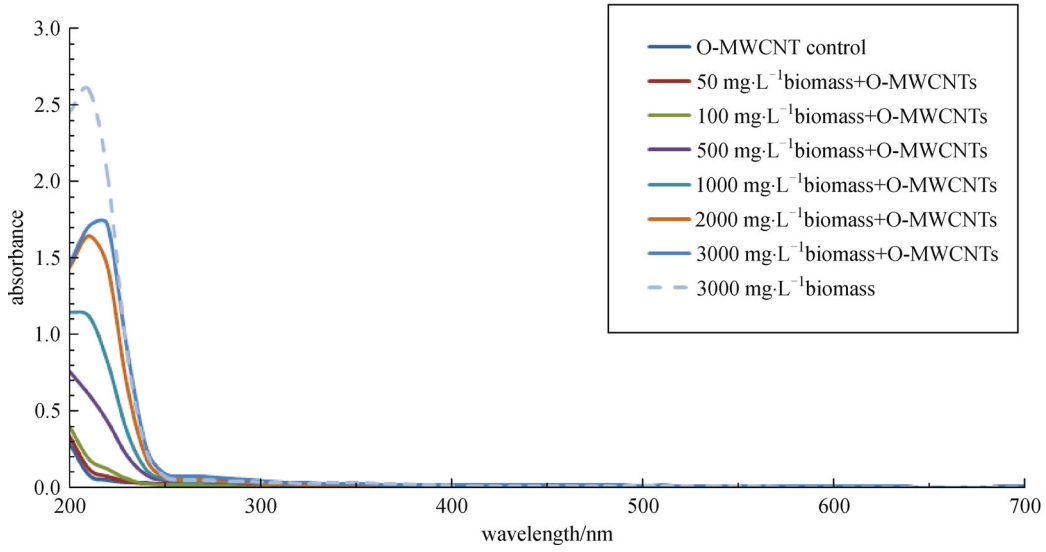

Fig. 2 UV-Vis scan of supernatant after biomass absorption on O-MWCNTs with 8.3% O. Initial O-MWCNT concentration is 25 mg $\cdot L^{-1}$. O-MWCNT control did not include biomass but only 25 mg O-MWCNT $\cdot L^{-1}$

MWCNTs decreased. Thus pristine and O- MWCNTs were nearly completely removed even without biomass. Nonetheless, the biomass experiments were performed to verify that the presence of biomass would not unexpectedly stabilize MWCNTs. For an initial O-MWCNT concentration of 25 mg $\cdot L^{-1}$, biomass concentrations ranging from 50 to 3,000 mg TSS $\cdot L^{-1}$ were added. Visual observations of the biomass and O-MWCNT solutions indicated complete removal of O-MWCNTs from the supernatant. UV-Vis spectroscopy confirmed the observations, measuring < 1 mg $\cdot L^{-1}$ MWCNTs in the supernatant at the end of the experiment. Greater than 96% removal of the O-MWCNTs with 8.3% oxygen was obtained even at the lower biomass application (50 mg $\cdot L^{-1}$). Because O-MWCNT suspension with 8.3% of oxygen is the most stable among five types of MWCNTs, it was concluded that $> 96\%$ removal would be achieved in the simulated wastewater treatment teats for all the MWCNTs, including the pristine one, and that the presence of biomass did not hinder MWCNT removal.

Previous research reports a critical aggregation concentration values for MWCNTs as 25 mmol $\cdot L^{-1}$ NaCl, 2.6 mmol $\cdot L^{-1}$ $CaCl_2$, and1.5 mmol $\cdot L^{-1}$ $MgCl_2$ at pH 6.0±0.2, in a time period ranging from 20 min to 3 h [24], whereas we observed this to occur at less than 1 mmol $\cdot L^{-1}$ $NaHCO_3$ matrix (pH = 7.0, ionic strength = 1 mmol $\cdot L^{-1}$) in shorter than 5 min. Nearly all wastewaters have ionic strengths above 1 mmol $\cdot L^{-1}$, thus higher ionic strength in wastewater can lead to more rapid homo- or hetero-aggregation of MWCNTs with other colloids because of the dependence of electrostatic repulsion on the Debye layer thickness [25]. In the prior study [24], the MWCNT suspension used in previous research was sonicated for 30 min, settled solids were removed, and the supernatant was used and re-sonicated – a process repeated five times [24]. This process may have significantly altered the size or surface functionality of the MWCNTs compared to this study where the pristine and O-MWCNTs were sonicated in a water bath only to form a homogeneous dispersion. Thus, different formulations of MWCNT suspensions may experience different rates of homo-aggregation or hetero-aggregation with biomass. Because homo-aggregation rates depend upon the initial NM concentration, it is possible the rate of aggregation at lower MWCNT concentration could be much lower than the rate observed in our experiments with 25 mg $\cdot L^{-1}$. To work with lower MWCNT concentrations in the presence of biomass would necessitate improved analytical detection of MWCNTs dispersed in solution.

The 1-h sonication can decrease the length of O-MWCNTs. Our unpublished data and other literatures also suggested the sonication could decrease the size of CNTs and unalter the surface oxidation state in the absence of strong oxidant [16,17,26]. However, even with decreased lengths of pristine MWCNTs and O-MWCNTs, 96% of them were removed from liquid phase after 3-h mixing and 0.5-h settling. Since sonication increased the stability of all MWCNT suspensions (upon observation), it is reasonably to conclude that more than 96% of pristine and O-MWCNTs could be removed from liquid phase with or without sonication.

3.3 Removal of graphene oxide by wastewater biomass

Unlike pristine or O-MWCNTs, GO did not undergo any measurable homo-aggregation in control experiments (i.e., no biomass). Addition of biomass led to lower GO concentrations in the supernatant (Fig. 3). Less than 10% removal of GO occurs at 50 or 100 mg $\cdot L^{-1}$. Biomass

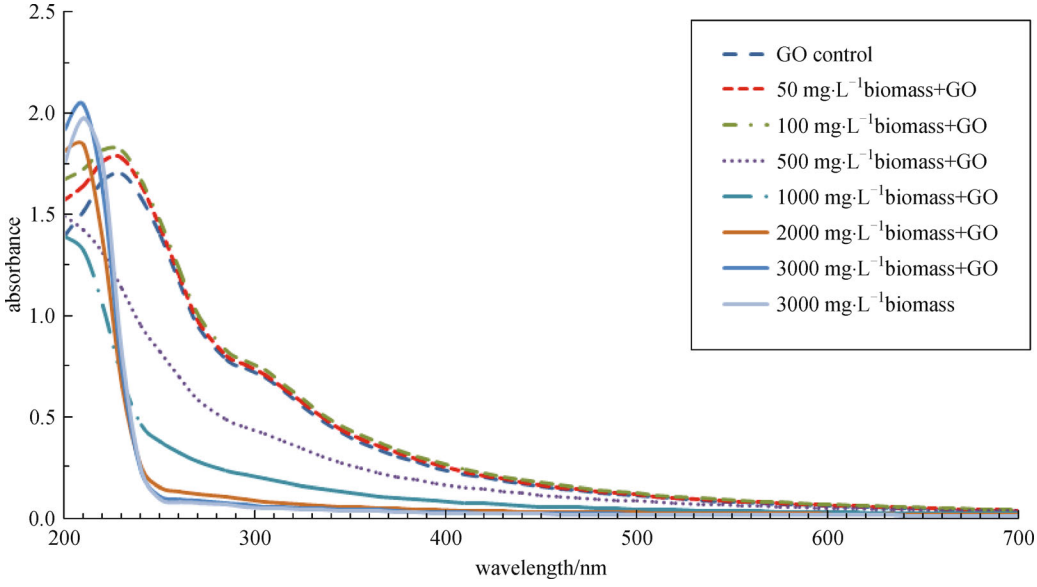

Fig. 3 UV-Vis scan of supernatant after biomass absorption on graphene oxide (GO). Initial GO concentration is 25 mg·L^{-1}. GO control did not include biomass but only 25 mg GO·L^{-1}

dosages of 500 and 1,000 mg·L^{-1} had 38% and 65% removal respectively. For biomass dosages above 2,000 mg TSS·L^{-1}, greater than 75% of GO was removed from the supernatant (compared against controls of GO without biomass). When the biomass concentration was below 100 mg TSS·L^{-1}, we could still find the characteristic absorption peak of GO at 230 nm. As biomass concentration increased, more GO was removed. At higher concentrations of biomass, the absorption peak of GO at 230 nm disappeared and the high concentration of biomass led to another peak at 215 nm (comparable to 3,000 mg ·L^{-1} biomass control).

Data for GO removal as a function of biomass dosage were fit using the Freundlich model (Fig. 4). By applying the Freundlich model, we did not assume equilibrium or any other thermodynamic state, but we simply applied the model as a mathematical fit of the data. Similar work has been applied elsewhere for NMs [26], oxo-anions, and other pollutants [27]. The Freundlich model ($q = 5.0\ C_s^{0.5}$) fit the observed data ($R^2 = 0.55$), where C_s is the supernatant concentration of GO and q represents a sorption density (mg GO·g TSS^{-1}).

To explore the dominant interaction between GO and biomass, the total surface area of GO and bacteria in biomass was calculated. Our previous results using QPCR [28] show the total bacteria is approximately 1.0×10^9 cells·mL^{-1} and the total archaea is approximately 1.0×10^7 cells·mL^{-1} in the biomass of 3,000 mg TSS·L^{-1}. Assuming the each cell has a similar size to a *E.coli* cell, we can estimate the total surface area of microorganism for biomass by multiplying the number of cells with the surface area of a *E.coli* cell. As a rod-shaped *E.coli* cell has surface area of approximately 0.39 μm^2 (0.5 μm in width by 2 μm in length) [29], the total surface area of microbes is approximately 3.94 cm^2· mL^{-1} for 3,000 mg TSS·L^{-1}. Additionally, the low ionic strength of matrix (1 mmol·L^{-1} $NaHCO_3$) would unlikely lead to fold or aggregation of GO, since other literature reported 50 mmol·L^{-1} of copper ion (i.e., Cu^{2+}) and above would be able to cause folding and aggregation of GO [30]. Thus the total surface area of GO (surface area from information provided by manufacture, 1200 m^2·g^{-1}) can be proportionally calculated to be about 300 cm^2·mL^{-1}, which was much higher than that of biomass at 3,000 mg TSS·L^{-1}. Therefore, the interaction among GO NMs likely dominated in the distribution process, though the carboxyl and hydroxyl group on the surface of GO might hinder the aggregation of GO [31].

3.4 Few layer graphene removal by biomass

The suspension of FLG was relatively stable after 30-min water bath sonication, and there was virtually no settling of FLG after one hour. At the end of the experiments, FLG was measured in the settled biomass and compared with the MWCNT or GO that was quantified in the supernatant. Experiments with FLG were conducted with a constant biomass concentration of 50 mg TSS·L^{-1} (see above) and variable FLG concentrations. In these experiments, the percentage FLG removed was nearly constant across the range of FLG concentrations tested. FLG removal averaged 11±3% (range: 8% to 16%). Consequently, when the data were plotted and fit by a Freundlich model ($q = 2.2\ C_s^{1.1}$; $R^2 = 0.94$, Fig. 4), the model exponent is nearly unity, which indicates a linear distribution of FLG between the supernatant and biomass. This was somewhat unexpected unless the FLG completely covered the biomass

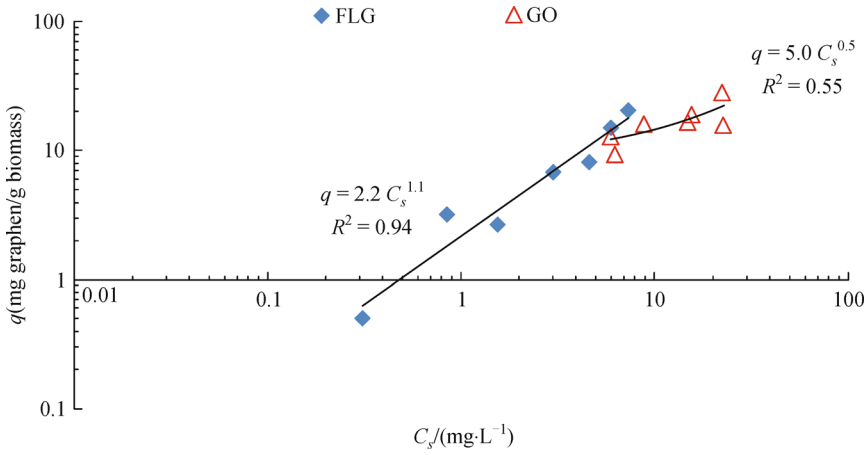

Fig. 4 Analysis using a Freundlich model of the supernatant NM (i.e., GO and FLG) concentrations (C_s, mg·L^{-1}) versus the amount of NM in the biomass (q, mg NM · mg TSS^{-1}). The initial concentration of GO was 25 mg·L^{-1} with varied biomass concentration (50 – 3,000 mg TSS·L^{-1}). The initial concentration of FLG was 0.3– 8.3 mg·L^{-1} with a fixed biomass concentration of 50 mg·L^{-1}

surface – even at the lowest FLG concentration – in which case the near unity exponent may represent interaction of FLG with similar FLG NMs orientated on the biomass surface. Fig.4 also clearly shows that more FLG can be removed by biomass compared to GO ($q_{FLG} > q_{GO}$), when C_s concentration was about 6–7 mg·L^{-1}.

A similar calculation was conducted on the total surface area of FLG NMs and bacteria in biomass, to examine the dominant interaction in the suspension. As shown above, the total surface area of microbes in 3,000 mg TSS·L^{-1} biomass is 3.94 cm^2·mL^{-1}. Proportionally, 50 mg TSS·L^{-1} biomass will have a surface area of approximately 6.56 × 10^{-2} cm^2·mL^{-1}. The total surface area in 0.3 mg·L^{-1} FLG (surface area, 21 m^2·g^{-1}) is approximately 63 cm^2·mL^{-1}, which is at least 100 fold larger than the surface area of microbes in 50 mg·L^{-1} biomass. Therefore, interaction of FLG with other FLG NMs likely occurred, and the aggregates of FLGs covered the surface of microbes in the biomass. These experiments raise a number of interesting mechanistic questions that will be investigated in the future. With the current data set, we can conclude quantitatively that > 84% of the FLG was removed by 50 mg TSS·L^{-1} of biomass. It is reasonable to expect FLG removal would increase at higher biomass concentrations, but current analytical methods limit these quantitative assessments.

3.5 Removal of carbonaceous nanomaterials by biomass

Table 1 summarizes the percentage removal by wastewater biomass of common carbonaceous NMs, including MWCNTs, FLGs, GO, fullerene, and functionalized fullerene. Except GO and functionalized fullerene, all other carbonaceous NMs could have more than 96% removal in the presence of 1,000 mg·L^{-1} biomass. GO removal was 65% with an initial concentration of 25 mg GO·L^{-1}and a biomass concentration of 1,000 mg·L^{-1}. Functionalized fullerene (initial concentration as 3 mg C ·L^{-1}) has a 14% of removal in the presence of 400 mg·L^{-1} biomass. Previous results indicate the surface functionalization/oxidation could affect the stability and removal rates of carbon nanomaterials in biomass absorption process [3,19].

The specific mechanism governing biosorption of carbonaceous NMs on biomass is not clear yet, though the interaction between NMs and extracellular polymeric substances (EPS, one of most important sources of organic matters) is considered a driving force [19,34]. The EPS in the biomass contains a large portion of hydrophobic materials, which can enhance the stability of fullerene in the suspension [19]. EPS can increase the electrical or steric repulsion [35] when interacting with carbonaceous NMs containing organic functional group on the surface. Thus GO with carboxyl group [31] showed a lower removal rate from the bulk water phase. Further research is needed to elucidate how the absorption forces change with different functionalization on the surface of carbonaceous NMs.

4 Conclusions

This study of pristine and O- MWCNTs, GO, and FLG in presence of biomass showed different removal from the water phase. Biomass at 1,000 mg·L^{-1} removed at least 65% of GO and 96% of pristine and O-MWCNTs with an initial concentrations of 25 mg C·L^{-1}, while biomass at 50 mg·L^{-1} remove 16% of FLG with an initial concentration of 1 mg C·L^{-1}. Because activated sludge in WWTP ranges from 1,000 mg·L^{-1} to 5,000 mg·L^{-1}, it can be concluded that majority of carbonaceous NMs entering into WWTPs would associate with biomass and be removed from the water phase. Analytical challenges still exist for quantify-

Table 1 Percentage removal of nanomaterials by the wastewater biomass

nanomaterials	diameter of NMs /(nm)	initial concentration of NMs/(mg·L^{-1})	biomass concentration /(mg·L^{-1})	percentage removal	references
multi-walled CNTs with 0.4% –8.3% oxygen	12	25	1,000	> 96%	this study
graphene oxide (GO)	1.1[a)]	25	1,000	65%	this study
few Layer Graphene (FLG)	10 – 20[a)]	1	50	16%	this study
fullerene (aq-nC$_{60}$)	88	4	400	90%	[19]
functionalized fullerene (nC$_{60}$(OH)$_x$)	48	12	400	14%	[19]
fullerene	88	0.07–2	500–2,000	95%	[32]
CNTs				90% –97% [b)]	[8]
general nanomaterials				32% –77% [b)]	[33]

Note: a) Represents thickness of NMs; b)represents assumed value used in modeling

ing pristine and O-MWCNTs and GO in the presence of high concentration of biomass. Further study is needed to address the analytical challenges of quantifying GO and MWCNTs in environmental matrices.

Acknowledgements This study was funded by the US National Science Foundation (CBET 0847710) and US Environmental Protection Agency (RD8355800). Any opinions, findings, and conclusions or recommendations expressed in this material are those of the author(s) and do not necessarily reflect the views of the funding agencies. We are grateful to Dr. Howard Fairbrother at Johns Hopkins University, who kindly provided us five types of MWCNTs for use in this study.

References

1. U.S.EPA. Comprehensive Environmental Assessment Applied to Multiwalled Carbon Nanotube Flame-Retardant Coatings in Upholstery Textiles: A Case Study Presenting Priority Research Gaps for Future Risk Assessments (Final Report). U.S. Environmental Protection Agency, Washington, D C: 2013
2. Baur J, Silverman E. Challenges and opportunities in multifunctional nanocomposite structures for aerospace applications. MRS Bulletin, 2007, 32(04): 328–334
3. Petersen E J, Zhang L, Mattison N T, O'Carroll D M, Whelton A J, Uddin N, Nguyen T, Huang Q, Henry T B, Holbrook R D, Chen K L. Potential release pathways, environmental fate, and ecological risks of carbon nanotubes. Environmental Science & Technology, 2011, 45(23): 9837–9856
4. Piccinno F, Gottschalk F, Seeger S, Nowack B.Industrial production quantities and uses of ten engineered nanomaterials in Europe and the world. Journal of Nanoparticle Research, 2012, 14(9): 1–11
5. Hendren C O, Mesnard X, Dröge J, Wiesner M R. Estimating production data for five engineered nanomaterials as a basis for exposure assessment. Environmental Science & Technology, 2011, 45(7): 2562–2569
6. Clark S, Mallick G G. Global graphene market (product type, application, geography)—size, share, global trends, company profiles, demand, insights, analysis, research, report, opportunities, segmentation and forecast, 2013–2020. Allied Market Research, 2014
7. Nowack B, David R M, Fissan H, Morris H, Shatkin J A, Stintz M, Zepp R, Brouwer D. Potential release scenarios for carbon nanotubes used in composites. Environment International, 2013, 59: 1–11
8. Mueller N C, Nowack B. Exposure modeling of engineered nanoparticles in the environment. Environmental Science & Technology, 2008, 42(12): 4447–4453
9. Gottschalk F, Sonderer T, Scholz R W, Nowack B. Modeled environmental concentrations of engineered nanomaterials (TiO_2, ZnO, Ag, CNT, Fullerenes) for different regions. Environmental Science & Technology, 2009, 43(24): 9216–9222
10. U.S.EPA. Interim Technical Guidance for Assessing Screening Level Environmental Fate and Transport of, and General Population, Consumer, and Environmental Exposure to Nanomaterials 2010. Office of Pollution Prevention and Toxics (OPPT), U.S. Environmental Protection Agency, Washington, D C: 2011
11. Herrero-Latorre C, Álvarez-Méndez J, Barciela-García J, García-Martín S, Peña-Crecente R M. Characterization of carbon nanotubes and analytical methods for their determination in environmental and biological samples: a review. Analytica chimica acta, 2015, 853: 77–94
12. Plata D L, Reddy C M, Gschwend P M. Thermogravimetry-mass spectrometry for carbon nanotube detection in complex mixtures. Environmental Science & Technology, 2012, 46(22): 12254–12261
13. Doudrick K, Herckes P, Westerhoff P. Detection of carbon nanotubes in environmental matrices using programmed thermal analysis. Environmental Science & Technology, 2012, 46(22): 12246–12253
14. Doudrick K, Corson N, Oberdörster G, Eder A C, Herckes P, Halden R U, Westerhoff P. Extraction and quantification of carbon nanotubes in biological matrices with application to rat lung tissue. ACS Nano, 2013, 7(10): 8849–8856
15. Doudrick K, Nosaka T, Herckes P, Westerhoff P. Quantification of graphene and graphene oxide in complex organic matrices. Environmental Science: Nano, 2015, 2: 60–67
16. Smith B, Wepasnick K, Schrote K E, Cho H H, Ball W P, Fairbrother D H. Influence of surface oxides on the colloidal stability of multi-walled carbon nanotubes: a structure-property relationship. Langmuir, 2009, 25(17): 9767–9776
17. Yi P, Chen K L. Influence of surface oxidation on the aggregation

and deposition kinetics of multiwalled carbon nanotubes in monovalent and divalent electrolytes. Langmuir, 2011, 27(7): 3588–3599

18. Cho H H, Smith B A, Wnuk J D, Fairbrother D H, Ball W P. Influence of surface oxides on the adsorption of naphthalene onto multiwalled carbon nanotubes. Environmental Science & Technology, 2008, 42(8): 2899–2905
19. Kiser M A, Ryu H, Jang H, Hristovski K, Westerhoff P. Biosorption of nanoparticles to heterotrophic wastewater biomass. Water Research, 2010, 44(14): 4105–4114
20. APHA. AWWA, WEF. Standard Methods for the Examination of Water and Wastewater. 21st ed. American Public Health Association (APHA), the American Water Works Association (AWWA), and the Water Environment Federation (WEF), 2005
21. Grady J L C P, Daigger G T, Lim H C. Biological Wastewater Treatment. 2nd ed. Revised and Expanded ed. Florida: CRC Press, 1999
22. Shin H J, Kim K K, Benayad A, Yoon S M, Park H K, Jung I S, Jin M H, Jeong H K, Kim J M, Choi J Y, Lee Y H. Efficient reduction of graphite oxide by sodium borohydride and its effect on electrical conductance. Advanced Functional Materials, 2009, 19(12): 1987–1992
23. Zhang J, Yang H, Shen G, Cheng P, Zhang J, Guo S. Reduction of graphene oxide via L-ascorbic acid. Chemical Communications, 2010, 46(7): 1112–1114
24. Saleh N B, Pfefferle L D, Elimelech M. Aggregation kinetics of multiwalled carbon nanotubes in aquatic systems: measurements and environmental implications. Environmental Science & Technology, 2008, 42(21): 7963–7969
25. Suzuki K, Tanaka Y, Osada T, Waki M. Removal of phosphate, magnesium and calcium from swine wastewater through crystallization enhanced by aeration. Water Research, 2002, 36(12): 2991–2998
26. Wiesner M R, Bottero J Y. A risk forecasting process for nanostructured materials, and nanomanufacturing. Comptes Rendus Physique, 2011, 12(7): 659–668 (in German)
27. Westerhoff P, Nowack B. Searching for global descriptors of engineered nanomaterial fate and transport in the environment. Accounts of Chemical Research, 2013, 46(3): 844–853
28. Yang Y, Chen Q, Wall J D, Hu Z. Potential nanosilver impact on anaerobic digestion at moderate silver concentrations. Water Research, 2012, 46(4): 1176–1184
29. Neidhardt F C. Escherichia coli and Salmonella: Cellular and Molecular Biology. Washington, D C: ASM Press, 1996
30. Yang S T, Chang Y, Wang H, Liu G, Chen S, Wang Y, Liu Y, Cao A. Folding/aggregation of graphene oxide and its application in Cu^{2+} removal. Journal of Colloid and Interface Science, 2010, 351 (1): 122–127
31. He H, Klinowski J, Forster M, Lerf A. A new structural model for graphite oxide. Chemical Physics Letters, 1998, 287(1–2): 53–56
32. Wang Y, Westerhoff P, Hristovski K D. Fate and biological effects of silver, titanium dioxide, and C_{60} (fullerene) nanomaterials during simulated wastewater treatment processes. Journal of Hazardous Materials, 2012, 201–202(0): 16–22
33. Keller A A, Lazareva A. Predicted releases of engineered nanomaterials: from global to regional to local. Environmental Science & Technology Letters, 2014, 1(1): 65–70
34. Chen K L, Elimelech M. Relating colloidal stability of fullerene (C_{60}) nanoparticles to nanoparticle charge and electrokinetic properties. Environmental Science & Technology, 2009, 43(19): 7270–7276
35. Becker W C, Foundation A R. Using Oxidants to Enhance Filter Performance. AWWA Research Foundation and American Water Works Association, 2004